

Shear failure of beams: experiments and analysis

Autor(en): **Van den Beukel, A. / Blaauwendraad, J. / Merks, P.J.G.**

Objekttyp: **Article**

Zeitschrift: **IABSE reports of the working commissions = Rapports des commissions de travail AIPC = IVBH Berichte der Arbeitskommissionen**

Band (Jahr): **34 (1981)**

PDF erstellt am: **22.05.2024**

Persistenter Link: <https://doi.org/10.5169/seals-26911>

Nutzungsbedingungen

Die ETH-Bibliothek ist Anbieterin der digitalisierten Zeitschriften. Sie besitzt keine Urheberrechte an den Inhalten der Zeitschriften. Die Rechte liegen in der Regel bei den Herausgebern.

Die auf der Plattform e-periodica veröffentlichten Dokumente stehen für nicht-kommerzielle Zwecke in Lehre und Forschung sowie für die private Nutzung frei zur Verfügung. Einzelne Dateien oder Ausdrucke aus diesem Angebot können zusammen mit diesen Nutzungsbedingungen und den korrekten Herkunftsbezeichnungen weitergegeben werden.

Das Veröffentlichen von Bildern in Print- und Online-Publikationen ist nur mit vorheriger Genehmigung der Rechteinhaber erlaubt. Die systematische Speicherung von Teilen des elektronischen Angebots auf anderen Servern bedarf ebenfalls des schriftlichen Einverständnisses der Rechteinhaber.

Haftungsausschluss

Alle Angaben erfolgen ohne Gewähr für Vollständigkeit oder Richtigkeit. Es wird keine Haftung übernommen für Schäden durch die Verwendung von Informationen aus diesem Online-Angebot oder durch das Fehlen von Informationen. Dies gilt auch für Inhalte Dritter, die über dieses Angebot zugänglich sind.



Shear Failure of Beams: Experiments and Analysis

Rupture par effort tranchant de poutres: essais et analyse

Schubversagen von Balken: Versuch und Berechnung

A. VAN DEN BEUKEL

Research engineer
IBBC-TNO
Rijswijk, Holland

J. BLAAUWENDRAAD

Prof. dr. ir.
Rijkswaterstaat
Utrecht, Holland

P.J.G. MERKS

Research member
Rijkswaterstaat
Utrecht, Holland

TH. MONNIER

Senior Research engineer
IBBC-TNO
Rijswijk, Holland

SUMMARY

The results of experimental investigations into the ultimate strength of tunnels under combined action of bending and shear are used to verify the MICRO/1 program.

This program has been developed to analyze structures whose failure is strongly dominated by one or a few discrete cracks. The results of the analysis even enrich the insight which was gained by the experiments.

RÉSUMÉ

Les résultats de recherches expérimentales concernant la résistance à la rupture de tunnels soumis à l'action simultanée de flexion et de cisaillement sont utilisés pour vérifier le programme MICRO 1.

Ce programme a été développé pour l'analyse de structures dont la rupture est déterminée par quelques fissures distinctes. Les résultats de l'analyse enrichissent d'ailleurs la compréhension du phénomène observé lors des essais en laboratoire.

ZUSAMMENFASSUNG

Die Ergebnisse von Traglastversuchen an Tunneln unter gleichzeitiger Wirkung von Biegung und Querkraft wurden zur Prüfung des Programms MICRO/1 benutzt. Dieses Programm wurde für die Berechnung von Konstruktionen entwickelt, deren Versagen sehr stark von Einzelrissen beeinflusst wird. Die Rechenergebnisse haben die Einsicht in das Verhalten beim Versuch sehr vergrößert.



1. INTRODUCTION

Reinforced concrete beams which fail in shear show at failure one or a few dominating cracks. Finite element programs using the concept of "smeared cracks" do not cover such types of problems in a proper way. The MICRO/1 program has been developed recently especially for such cases. At the same time Rijkswaterstaat, the Dutch State Public Works, and IBBC-TNO, the Institute TNO for Building Materials and Building Structures, co-operate in an investigation of the ultimate strength of tunnels for combinations of bending moment and shear force. This is a beam type problem for a uniformly distributed load. The first part of this paper reviews the experimental work of this study. The second part of the paper enters into the analysis of some of the tested beams and discusses the potentialities and results. It appears that the insight, which is gained from the experimental work, will get enriched by the detailed information of an analysis at a rather micro-level.

2. EXPERIMENTAL WORK

The experiments are part of a study on the shear-strength of reinforced concrete structures like tunnels, especially with the object to improve the design procedure. The load considered is uniformly distributed. Figure 2.1 being a picture of a tunnel-section on scale after testing, indicates one of the regions of special interest.

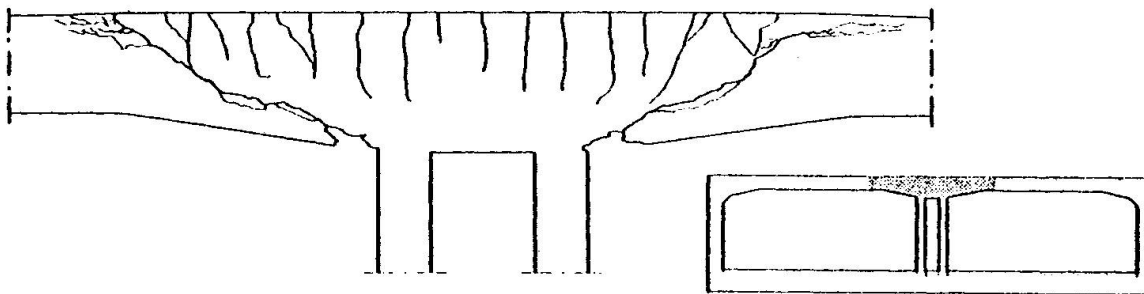


Fig. 2.1 Part of a tunnel-section after testing

The experimental investigation has rather a wide scope and concerns the influence on the shear-strength of reinforced concrete of:

- the ratio between moment and shear force;
- a low percentage of longitudinal reinforcement;
- varying depth of the structure;
- normal force;
- stirrup reinforcement.

An appropriate test-specimen has been developed for the experiments as shown in figure 2.2. In this set up of the tests a certain ratio between moment and shear force can be adjusted by choosing the right values for the sizes a , e and l as indicated in figure 2.2. The test specimen were loaded uniformly distributed by means of hoses which were inflated by waterpressure. Loads, deformation and crack formation were recorded.

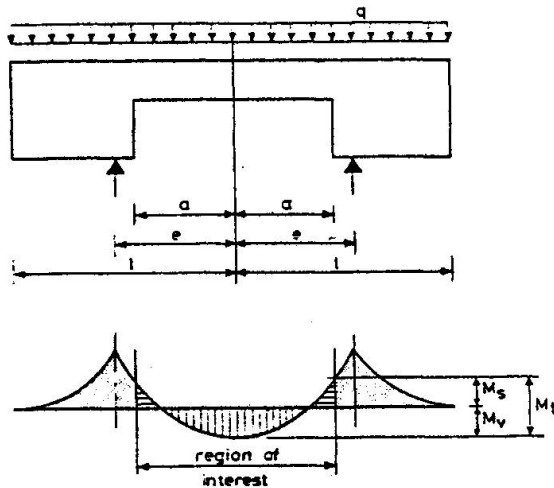


Fig. 2.2 Test-specimen

The decision on specific series of test-specimen was supported by the result of the study of data from literature. With that information an empirical formula has been developed for the shear strength as a function of the concrete strength f_c , the percentage of longitudinal reinforcement ω_0 , the normal force N and the ratio between moment M and shear force T by means of the term $\frac{T \cdot h}{M}$ (h = effective depth of the cross-section).

Following literature, difference was made between diagonal tension failure (with shear T_1) and shear compression failure (with shear T_2), resulting in:

$$T_1 = \tau_1 \cdot bh = (1 + 1.2 \frac{T \cdot h}{M}) bh \cdot f\{f_c, \omega_0, N\}$$

$$T_2 = \tau_2 \cdot bh = \frac{T \cdot h}{M} \cdot bh \cdot g\{f_c, \omega_0, N\}$$

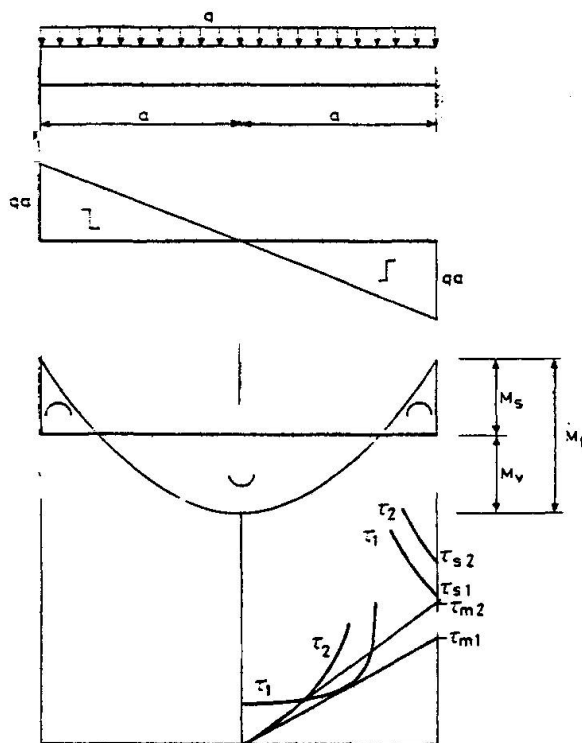


Fig. 2.3 Calculations of shear strength



Most of the experiments in literature are carried out with concentrated loads.

In these cases the ratio $\frac{T h}{M}$ can be expressed in terms of sizes, the slenderness a/h in which a is the distance between the concentrated load and the nearest support.

By means of the formulas mentioned, the shear strength of an element can be evaluated as illustrated in figure 2.3. In this case T_{m1} (the nominal shear stress), the extrapolation of the diagonal tension strength in the span determines the maximum shear force in the element at ultimate.

The series of test-specimen for the experimental investigation have been chosen in such a way that the area of practical interest would be covered. As far as the study on the influence of the moment/shear force ratio is concerned, 3 series of test-specimen were designed:

- serie A with $a/h = 3$
- serie B $a/h = 4,5$
- serie C $a/h = 6$

In each of the series 5 values of $\alpha = \frac{M_v}{M_t}$ have been investigated namely

$\alpha = 0, 0.25, 0.50, 0.75$ and 1.0 . Those test-specimen had no stirrup-reinforcement, the percentage of longitudinal reinforcement amounts $\omega_0 = 2\%$. Two of the results of those tests will be considered further here by means of calculations with the MICRO/1 program. It concerns the elements B2 and B4. The element B2 has a slenderness $a/h = 4.5$ and a moment distribution determined by $\alpha = 0.25$. The shear strength near the clamped support governs the bearing capacity. Figure 2.4 shows the evaluation of the shear strength. The expected maximum shear force was $T_u = 63.7$ kN. Because a part of the uniformly distributed load will be carried down directly to the support, the line indicating T_2 at the support can be replaced over a certain distance $x = 0.5 M_s/T_s$ as indicated in fig. 2.4 by a horizontal dotted line. The maximum shear force at ultimate in the test amounts 66.5 kN. After failure, this side of the element has been repaired and strengthened. At the other side of the element an ultimate maximum shear force of 78.4 kN was attainable. Failure occurred after a gradual development of the crack pattern. At ultimate the concrete compression diagonal in the area of negative moments near the supports split suddenly.

The element B4 has a slenderness $a/h = 4.5$ and a moment-distribution determined by $\alpha = 0.75$. The shear strength of this element in the region of the span governs the bearing capacity. Figure 2.5 shows the evaluation of the shear strength. The expected maximum shear force was $T_u = 52.9$ kN. The maximum shear force reached in the test was 52 kN. After failure on one side of the element this region has been repaired and strengthened and testing has been proceeded after that. The other side in this case showed the same strength giving a maximum shear force at ultimate of 52 kN. Failure occurred where that was expected; the mechanism appeared rather suddenly along a main crack more or less connecting cracks from lower load stages.

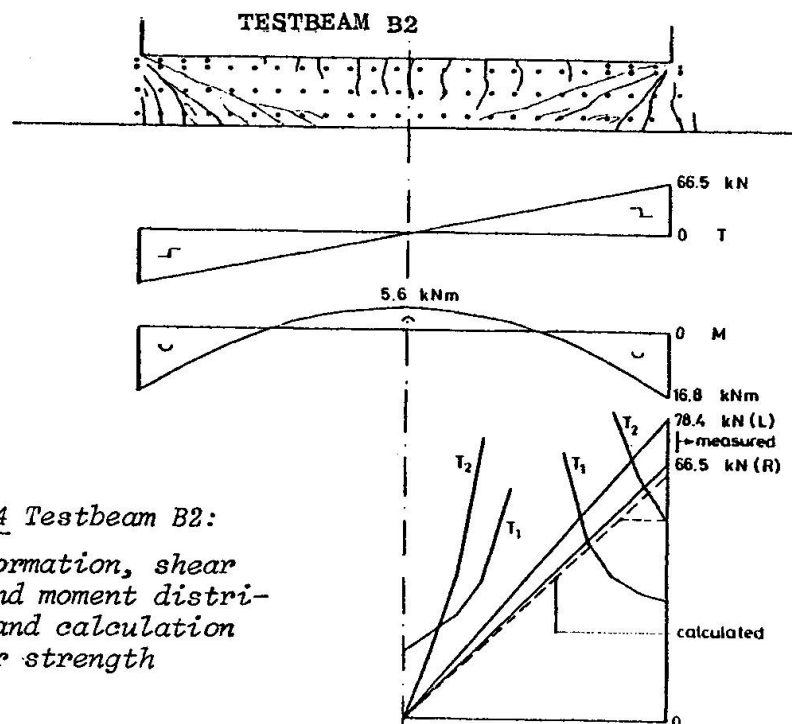


Fig. 2.4 Testbeam B2:

Crack-formation, shear force and moment distribution and calculation of shear strength

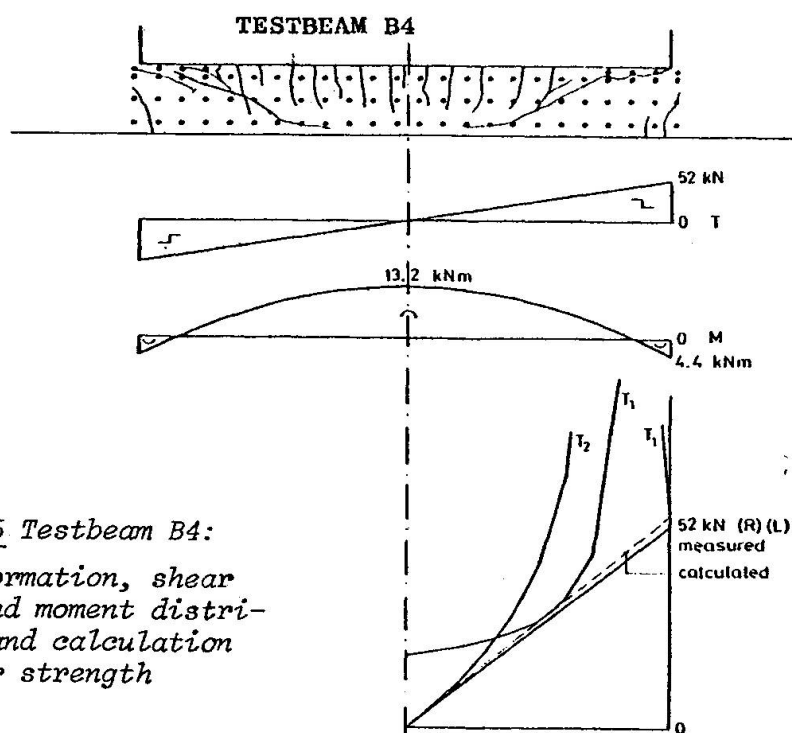


Fig. 2.5 Testbeam B4:

Crack-formation, shear force and moment distribution and calculation of shear strength

One of the conclusions from this study on shear strength is, that within the span of the member T_1 or T_2 is governing in accordance with prediction and shown. Near a clamped support a more favourable value T_2 is attainable in each case.



3. ANALYSIS

3.1. The MICRO/1 program

The program which is used for the analysis was developed in the frame-work of the Dutch joint research project 'Betonmechanica' [1]. The reader can find full details in HERON, 1981, nr. 1c by the authors H.J. Grootenboer, S.F.C.H. Leijten and J. Blaauwendraad. Here it is enough to recapitulate the following essential features:

- the program solves reinforced structures in plane stress.
- no 'smeared out' approach is used for cracking, but real discrete cracks can come into being and propagate, and may cross the element mesh irregularly.
- the aggregate interlock between the two faces of a crack is taken into account depending on the crack opening.
- bond and bondslip between concrete and reinforcement bars is taken into account. If a crack crosses a reinforcement bar, the discontinuous distribution of the bond stress is simulated.
- material data for concrete (crushing and cracking), reinforcement bond, aggregate interlock and dowel action account for nonlinearities, plasticity, hardening and softening, where applying.

The features listed here make this program particularly suited for the analysis of structures whose behaviour and failure is strongly influenced by one or a few dominating cracks. Beams which fail in shear typically belong to this category of problems.

3.2. Chosen beams and element mesh

The experimental investigations which have been discussed above, display a different type of failure in shear. Generally speaking two main types occur: the dominant crack at failure occurs somewhere along the span of the beam, or the dominant crack starts from the very end (the clamped end). In the latter case the crack is steeper than in the first case. The analysis reported here regards a simulation of each of the two main crack types. For this purposes the beams B2 and B4 have been selected (fig. 3.1) as described before. These beams have a similar slenderness but the ratio between the bending moment midspan and the total bending moment is different. The MICRO/1 program has been based on triangular elements for concrete and linear elements for the reinforcement bars. The modelling of the beams with aid of these elements is also shown in fig. 3.1, making use of symmetry. Supporting end blocks were added to the beam in order so to introduce the load, that the desired stress state in the beam will develop without disturbance. The analysis of beam B4 (ratio 0.75) had been started with the same mesh of beam B2 (ratio 0.25), but intermediate results of this analysis clearly indicated that the mesh should be refined in the compression zone at the clamped end, as is shown in the figure.

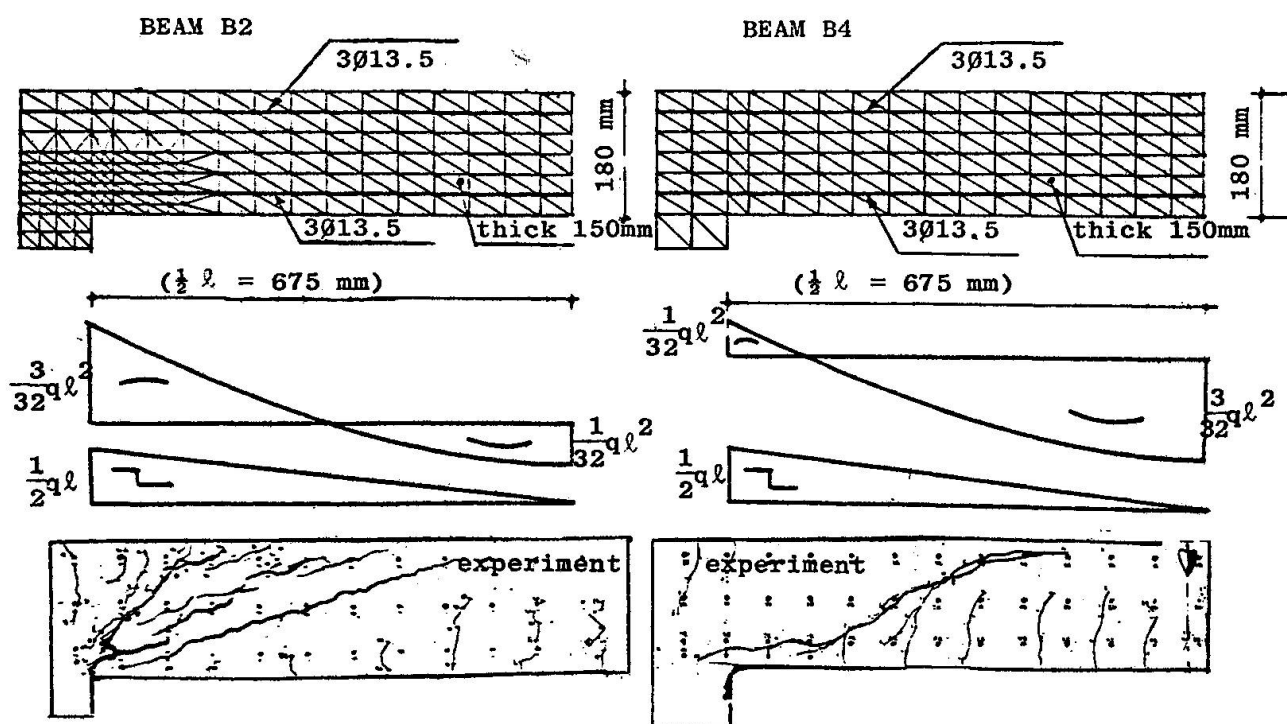


Fig. 3.1 Chosen beams and element mesh for verification of the MICRO/1 program

3.3. Material data

The material data listed in this section refer to the material models which have been presented in section 3.3 of [2].

Link's constitutive relations are used for the concrete, including crushing and cracking. The following data, taken from the relevant experiments, define the Link model and the cracking criterium:

Beam	$E(N/mm^2)$	$f_c(N/mm^2)$	$f_{ct}(N/mm^2)$
B2	27970	28.1	3.20
B4	27970	24.5	2.34

Aggregate interlock is accounted for in the following way. It is assumed that stresses normal to a crack will become zero, but shear stresses can occur in a crack. A rigid-plastic law is assumed for the relation between the shear stress τ and the parallel displacement of the two crack faces relative to each other $\Delta_{||}$. The limit value τ_{max} in this rigid-plastic law is assumed to decrease for increasing crack opening Δ_{\perp} (dilatancy). The following relation is used (see [2]):

$$\tau_{max} = \frac{1}{k \Delta_{\perp}}$$

From earlier calculations it appeared that a good value for the coefficient k is:

$$k = 0.05 \text{ m/N}$$



The reinforcement steel can be modelled as an ideal elasto-plastic material. The modulus of elasticity E_s and the yield strength f_y are:

$$E_s = 210\,000 \text{ N/mm}^2$$

$$f_y = 415 \text{ N/mm}^2$$

The bond behaviour is modelled by a relation between the bond slip Δ_b and the bond stress τ . A linear relationship holds with stiffness G_b until the bond stress reaches a limiting value f_b . A softening branch is defined using a factor k , see [2]. The following data yield from earlier comparisons:

$$G_b = 500 \text{ N/mm}^3$$

$$f_b = 5 \text{ N/mm}^2$$

$$k = 10 \text{ mm}^{-2}$$

The dowel action requires the specification of a relationship between normal stresses σ and a displacement Δ_d of the reinforcement bar relative to the concrete. An ideal elasto-plastic law is assumed, with a stiffness G_d and a limiting value f_d . The following data have been chosen:

$$G_d = 1 \text{ N/mm}^2$$

$$f_d = 20 \text{ N/mm}^2$$

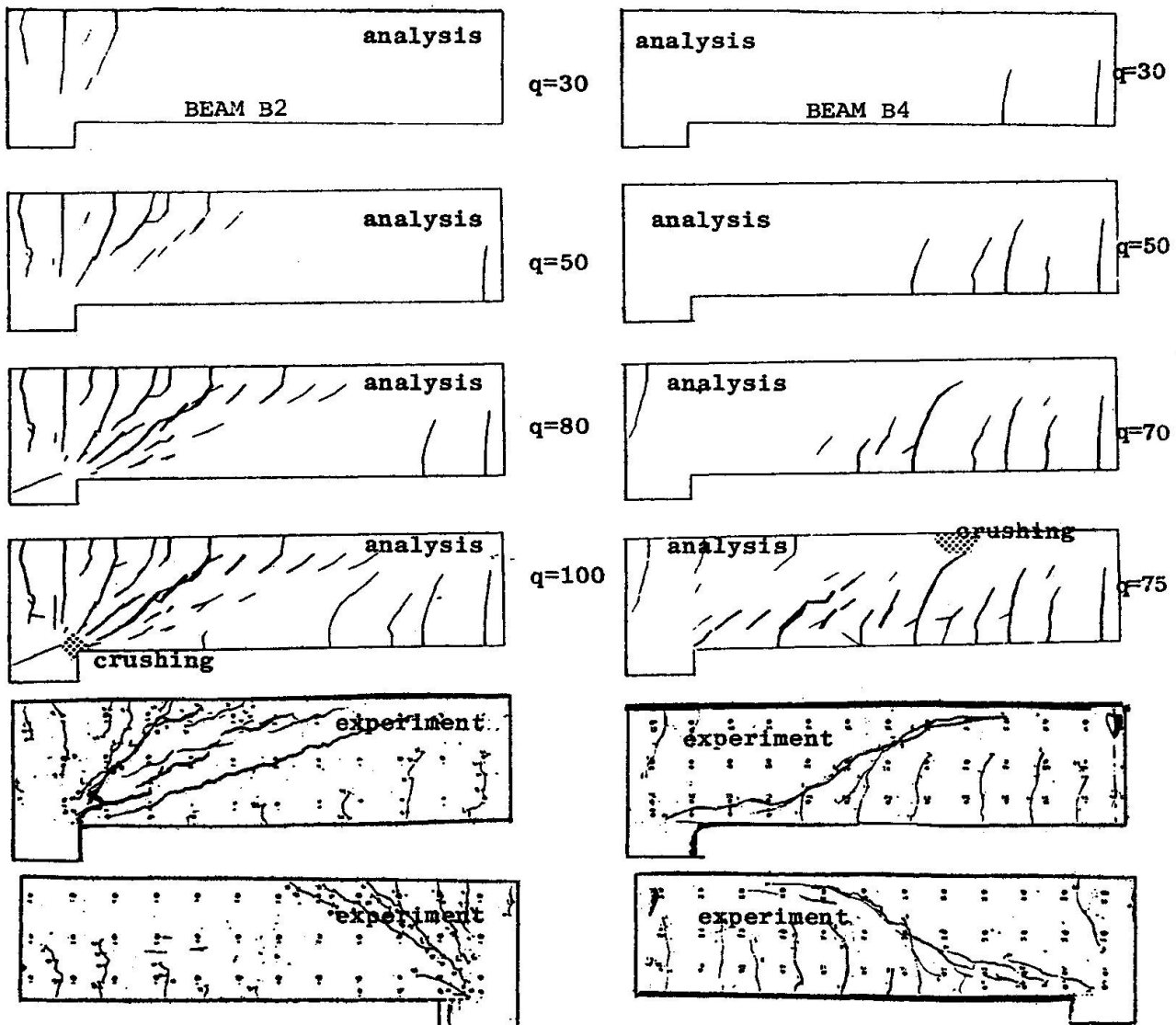


Fig. 3.2 Crack pattern in experiment and analysis for several load levels

3.4. Discussion of results

Crack pattern

The crack pattern for several load levels is shown in fig. 3.2. This figure is instructive as for the propagation of already existing cracks and the development of new ones. The thickness of lines in the analysis is a measure for the crack opening. It can be seen that initially all cracks start due to bending, but at higher load levels the cracks propagate or come into being under an inclination. Both beams start failing due to crushing in the compression zone. When we want compare the crack pattern in the analysis and the experiment, one should bear in mind that the final failure cracks spring up suddenly at the limit load level. For beam B2 these failure cracks accord pretty well with the crack pattern which had developed gradually during the loading process of the beam. In beam B4, however, a totally new crack comes into being in the very last second of the experiment which runs on top of all crack tips in the failure area. The MICRO/1 program is not able to calculate this very last crack phenomenon. Taking in account this fact, the agreement between the results of experiment and analysis is very satisfactory. We conclude: the two different patterns of cracking in beam B4 and beam B2, which showed up in the experiments, can be simulated by the MICRO/1 program.

Load-deflection curves

The agreement between experiment and analysis can be concluded also from the comparison of the load deflection curves in fig. 3.3. The displacement on the horizontal axis is the difference of the vertical displacement at midspan and at the support. In the experimental investigation this displacement was measured separately for the lefthand half of the span and for the righthand half of the span.

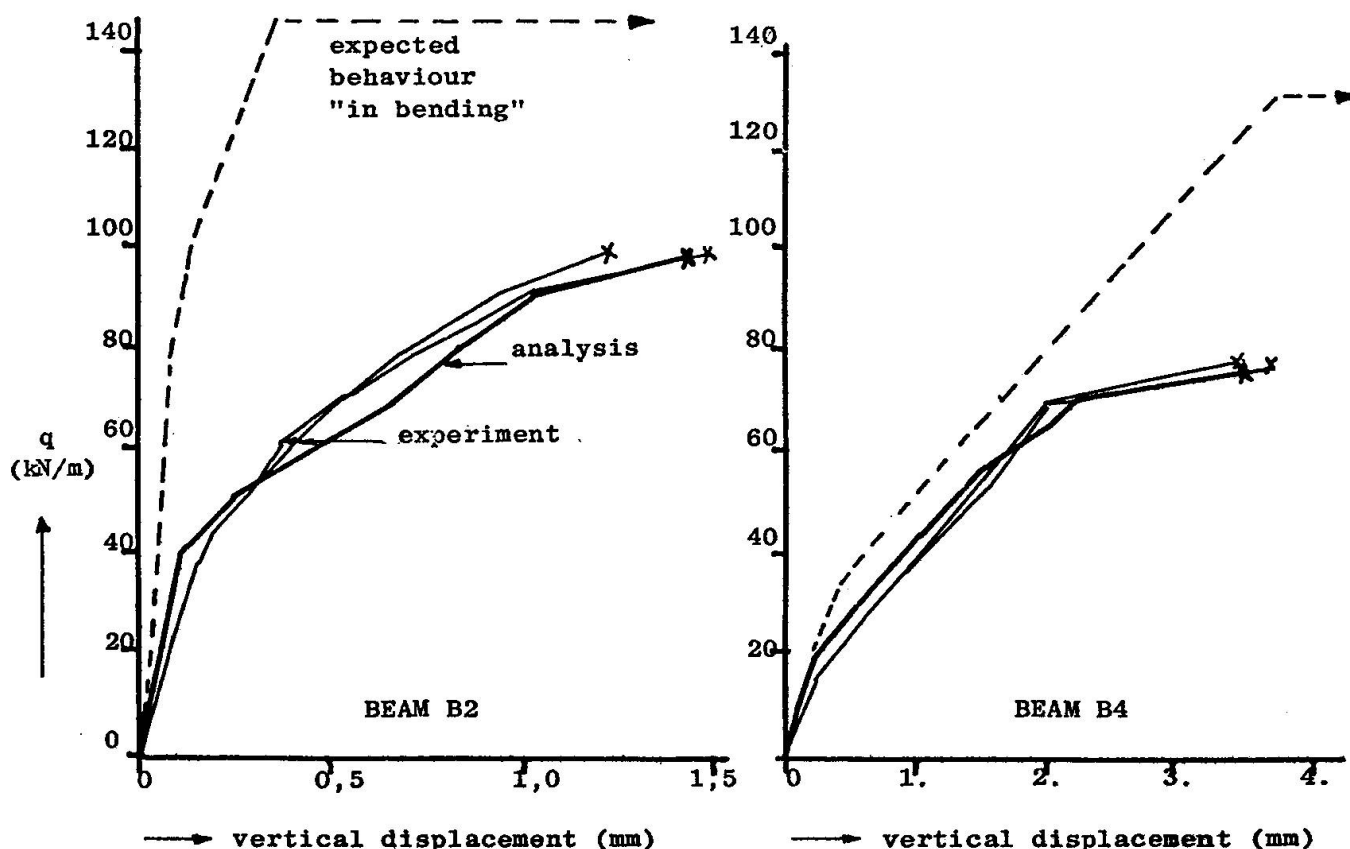


Fig. 3.3 Load deflection curves



The authors enjoyed the good agreement, especially for the ultimate value of the uniformly distributed load q in this figure. There is a noticeable difference between the behaviour of beam B2 and beam B4. The beam B2 shows a gradual decrease of stiffness during the loading process, whilst the beam B4 suddenly loses much stiffness in the last loading step. This difference also finds expression in the analysis. It can be explained with aid of the crack patterns of fig. 3.2. In beam B2 no new important cracks occur in the final loading stage between $q = 80$ kN/m and $q = 100$ kN/m, and the existing crack openings just grow something. In beam B4, however, a large number of new cracks develops in the final loading stage between $q = 70$ kN/m and $q = 75$ kN/m, one crack of which opens immediately very much. This explains the abrupt loss of stiffness.

The difference in behaviour of beam B2 and beam B4 appears once more when we compare the found load-deflection curves with the curve which is to be expected for the same beam in case sufficient web reinforcement was used to have the beam fail in bending. These curves have been calculated by the STANIL/1 program, which is described in [2] as well. Beam B4 behaves "in bending" and fails abruptly due to insufficient shear capacity. Beam B2 deviates from the "in bending" behaviour as soon as cracking starts occurring.

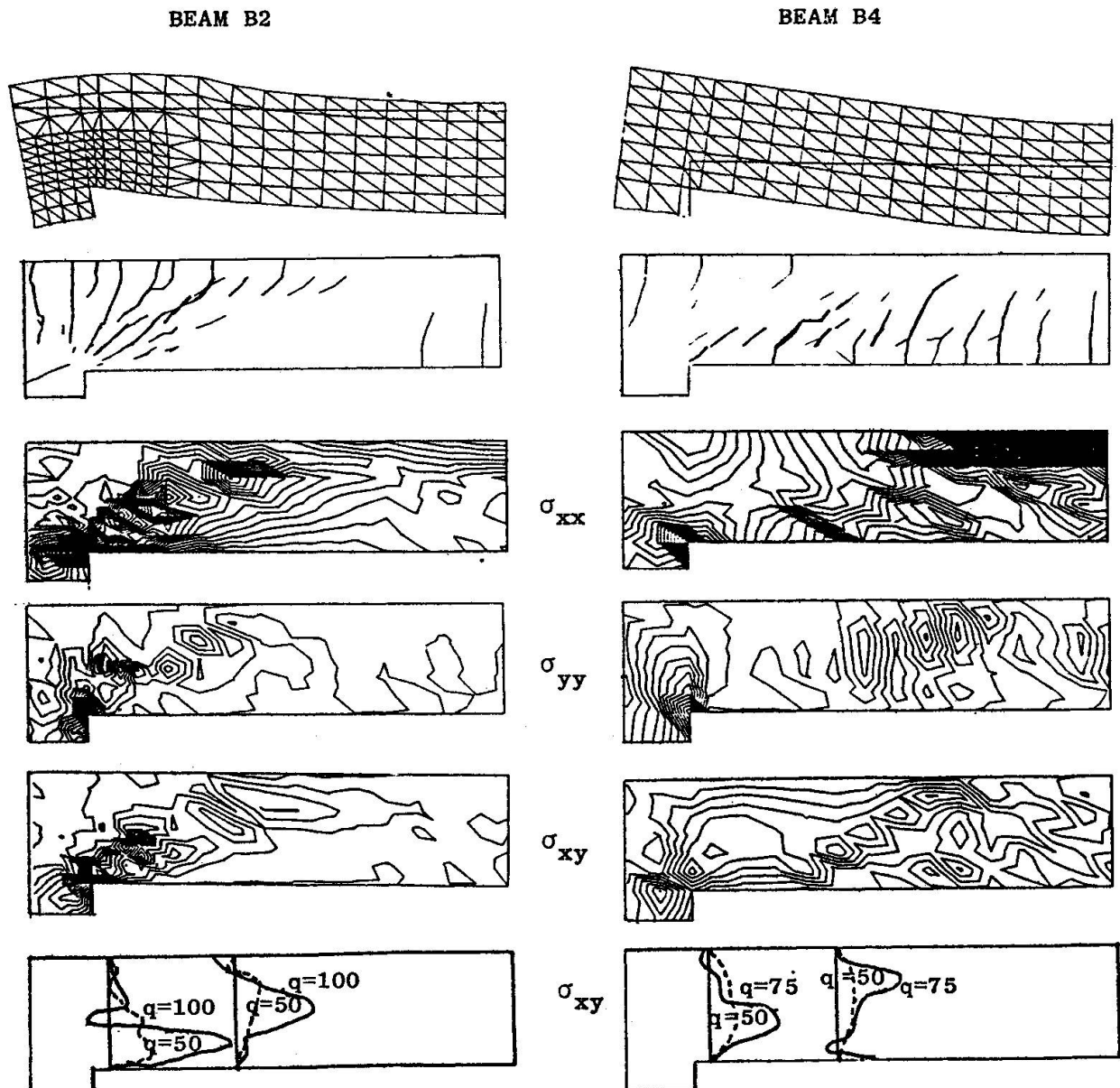


Fig. 3.4 Stress results from analysis

Stresses

In fig. 3.4 we show results for the stresses, together with the crack pattern and the deformed shape at the ultimate load. The stress plots are lines of constant value. Black areas occur for large gradients, which indicates stress concentrations. Such plots provide a quick view at the most interesting points. By hand we made a plot of the distribution of the shear stress at some interesting cross-sections which are self-explanatory in respect of the crack patterns. The stress in the reinforcement bars are plotted in fig. 3.5. The differences between the experimental results and the analysis results have been marked by a shaded area.

In both beams the point of zero stress value coincides for lower load levels with the position where the moment is zero. For higher loads this does not hold any longer, due to truss forming in the beam, which yields an increase of the reinforcement stress.

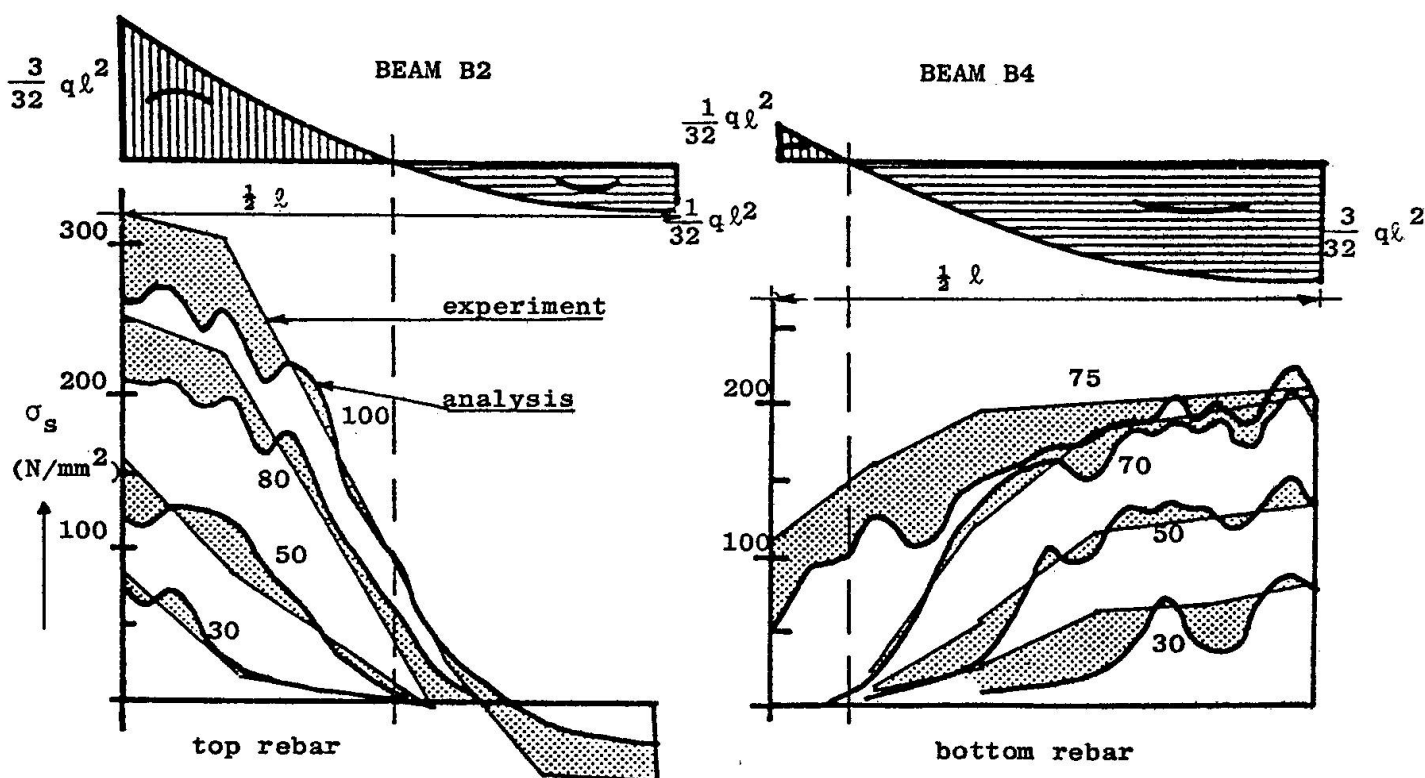


Fig. 3.5 Stresses in reinforcement bars for several load levels

4. CONCLUSION

The analysis of reinforced concrete beams without web reinforcement charged by uniformly distributed load yields results which are in close agreement with test results. The MICRO/1 program, handling discrete cracks, is capable of handling different types of shear failure in an appropriate way. If used complementary to experiments the analysis results will help understand the complete behaviour of the structure.



ACKNOWLEDGEMENT

The researchproject on shear capacity is jointly financed by Rijkswaterstaat and TNO-IBBC. The authors gratefully acknowledge the help and consult of ir. P. Kieft of Rijkswaterstaat, Department of Locks and Weirs, and of prof.Dr.Ing. H.W. Reinhardt and dr.ir. J.C. Walraven of Delft University of Technology, Department of Civil Engineering, in defining the research and in interpreting the results.

REFERENCES

1. Survey and Workplan of the joint project Betonmechanica, CUR-VB, 1977 Zoetermeer, The Netherlands.
2. GROOTENBOER, H.J.; LEIJTEN, S.F.C.H.; BLAAUWENDRAAD, J.: Concrete Mechanics; Numerical models for reinforced concrete structures in plane stress. Heron, 1980, no. 1c.